ATLAS measurements of CP violation and rare decay processes with beauty mesons

BEACH 2022 - 7 Jun 2022

Adam Barton on behalf of the ATLAS Collaboration

Introduction

- ATLAS detects huge amount of B hadrons 139 fb^{-1} of pp collisions at $\sqrt{s}$ = 13 TeV collected in 2015-2018 (Run 1: 25 fb^{-1} at 7 and 8 TeV).
- Producing 2.5M $b\bar{b}$ pairs/second, B_s, B_c, Λ_B, etc. available.
- **Triggering** is a challenge as luminosity increases, most of B-physics data selected by low-pT dimuon triggers.
- **Resolution** in m(μμ) : ~50 MeV at J/ψ mass, ~150 MeV at Υ(nS) masses, ~10 μm impact parameter resolution.
- **Time resolution** ~60 fs after installation of IBL in Run 2 (30% improvement w.r.t. Run 1).

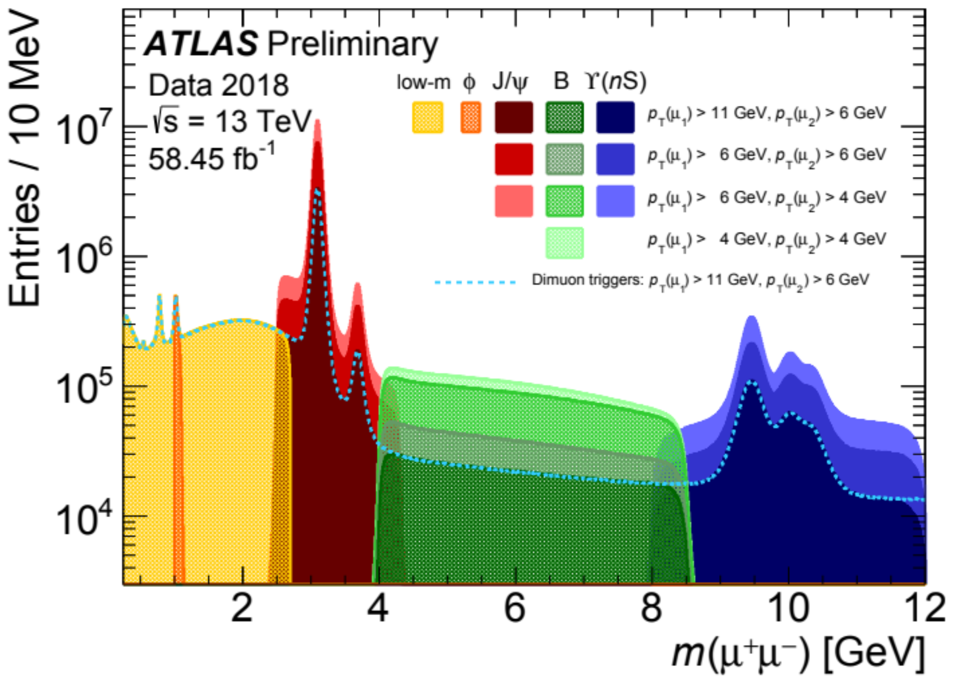

Eur. Phys. J. C 81 (2021) 342

Lancaster University

CPV in $B^0_s \rightarrow J/\psi\varphi$: Introduction

- The decay is expected to be sensitive to new physics via contributions to CP-violation.

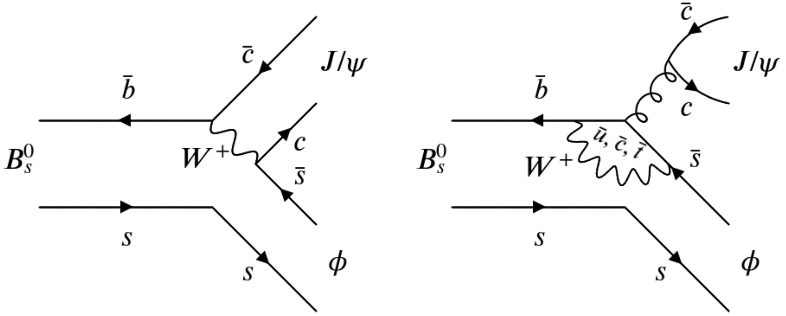

- Neutral B^0_s meson can oscillate into its antiparticle B^0_s (and vice versa). The oscillation frequency is characterized by the mass difference Δm_s of the heavy (B_H) and light (B_L) mass eigenstates.

- CP violation in interference of mixing and decay: the common final state is reached via two different decay chains:

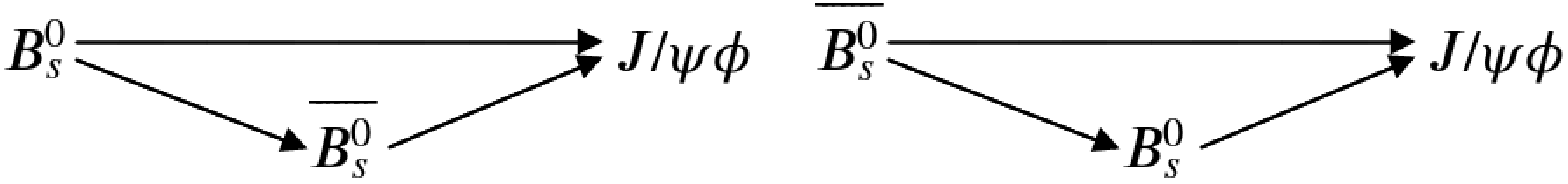

Eur. Phys. J. C 81 (2021) 342

CPV in $B^0_s \rightarrow J/\psi\phi$: Measurement

Lancaster University

- CP-violating phase is defined as the weak phase difference between the $B_s - \overline{B}_s$ mixing amplitude and the $b \rightarrow c\bar{c}s$ decay amplitude.
- In the Standard Model (SM) it can be related to the CKM matrix.

$$\phi_s = -0.03696^{+0.00072}_{-0.00082} \text{ rad}$$

- Any sizable deviation from this value would be a sign of beyond SM physics.
- Decay is pseudoscalar to vector-vector final state → admixture of CP-odd (L = 1) and CP-even (L = 0; 2) states. Distinguishable through time-dependent angular analysis.
- Non-resonant S-wave decay $B \rightarrow J/\psi K^+K^-$ and $B \rightarrow J/\psi f_0$ both contribute to the final state:
  - They are included in the differential decay rate.

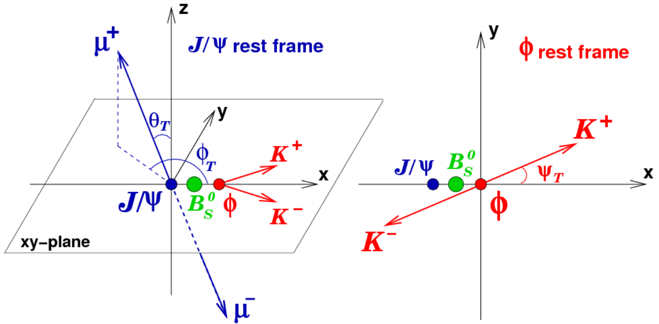

CPV in $B^0_s \to J/\psi\phi$: Measurement

k	$\mathcal{O}^{(k)}(t)$	$g^{(k)}(\theta_T, \psi_T, \phi_T)$
1	$\frac{1}{2}\lvert A_0(0)\rvert^2 \left[(1+\cos\phi_s)\,e^{-\Gamma_L^{(s)}t} + (1-\cos\phi_s)\,e^{-\Gamma_H^{(s)}t} \pm 2e^{-\Gamma_s t}\sin(\Delta m_s t)\sin\phi_s\right]$	$2\cos^2\psi_T(1-\sin^2\theta_T\cos^2\phi_T)$
2	$\frac{1}{2}\lvert A_\parallel(0)\rvert^2 \left[(1+\cos\phi_s)\,e^{-\Gamma_L^{(s)}t} + (1-\cos\phi_s)\,e^{-\Gamma_H^{(s)}t} \pm 2e^{-\Gamma_s t}\sin(\Delta m_s t)\sin\phi_s\right]$	$\sin^2\psi_T(1-\sin^2\theta_T\sin^2\phi_T)$
3	$\frac{1}{2}\lvert A_\perp(0)\rvert^2 \left[(1-\cos\phi_s)\,e^{-\Gamma_L^{(s)}t} + (1+\cos\phi_s)\,e^{-\Gamma_H^{(s)}t} \mp 2e^{-\Gamma_s t}\sin(\Delta m_s t)\sin\phi_s\right]$	$\sin^2\psi_T\sin^2\theta_T$
4	$\frac{1}{2}\lvert A_0(0)\rvert\lvert A_\parallel(0)\rvert\cos\delta_\parallel \left[(1+\cos\phi_s)\,e^{-\Gamma_L^{(s)}t} + (1-\cos\phi_s)\,e^{-\Gamma_H^{(s)}t} \pm 2e^{-\Gamma_s t}\sin(\Delta m_s t)\sin\phi_s\right]$	$\frac{1}{\sqrt{2}}\sin 2\psi_T\sin^2\theta_T\sin 2\phi_T$
5	$\lvert A_\parallel(0)\rvert\lvert A_\perp(0)\rvert \left[\frac{1}{2}(e^{-\Gamma_L^{(s)}t} - e^{-\Gamma_H^{(s)}t})\cos(\delta_\perp-\delta_\parallel)\sin\phi_s \pm e^{-\Gamma_s t}(\sin(\delta_\perp-\delta_\parallel)\cos(\Delta m_s t) - \cos(\delta_\perp-\delta_\parallel)\cos\phi_s\sin(\Delta m_s t))\right]$	$-\sin^2\psi_T\sin 2\theta_T\sin\phi_T$
6	$\lvert A_0(0)\rvert\lvert A_\perp(0)\rvert \left[\frac{1}{2}(e^{-\Gamma_L^{(s)}t} - e^{-\Gamma_H^{(s)}t})\cos\delta_\perp\sin\phi_s \pm e^{-\Gamma_s t}(\sin\delta_\perp\cos(\Delta m_s t) - \cos\delta_\perp\cos\phi_s\sin(\Delta m_s t))\right]$	$\frac{1}{\sqrt{2}}\sin 2\psi_T\sin 2\theta_T\cos\phi_T$
7	$\frac{1}{2}\lvert A_S(0)\rvert^2 \left[(1-\cos\phi_s)\,e^{-\Gamma_L^{(s)}t} + (1+\cos\phi_s)\,e^{-\Gamma_H^{(s)}t} \mp 2e^{-\Gamma_s t}\sin(\Delta m_s t)\sin\phi_s\right]$	$\frac{2}{3}\left(1-\sin^2\theta_T\cos^2\phi_T\right)$
8	$\alpha\lvert A_S(0)\rvert\lvert A_\parallel(0)\rvert \left[\frac{1}{2}(e^{-\Gamma_L^{(s)}t} - e^{-\Gamma_H^{(s)}t})\sin(\delta_\parallel-\delta_S)\sin\phi_s \pm e^{-\Gamma_s t}(\cos(\delta_\parallel-\delta_S)\cos(\Delta m_s t) - \sin(\delta_\parallel-\delta_S)\cos\phi_s\sin(\Delta m_s t))\right]$	$\frac{1}{3}\sqrt{6}\sin\psi_T\sin^2\theta_T\sin 2\phi_T$
9	$\frac{1}{2}\alpha\lvert A_S(0)\rvert\lvert A_\perp(0)\rvert\sin(\delta_\perp-\delta_S) \left[(1-\cos\phi_s)\,e^{-\Gamma_L^{(s)}t} + (1+\cos\phi_s)\,e^{-\Gamma_H^{(s)}t} \mp 2e^{-\Gamma_s t}\sin(\Delta m_s t)\sin\phi_s\right]$	$\frac{1}{3}\sqrt{6}\sin\psi_T\sin 2\theta_T\cos\phi_T$
10	$\alpha\lvert A_0(0)\rvert\lvert A_S(0)\rvert \left[\frac{1}{2}(e^{-\Gamma_H^{(s)}t} - e^{-\Gamma_L^{(s)}t})\sin\delta_S\sin\phi_s \pm e^{-\Gamma_s t}(\cos\delta_S\cos(\Delta m_s t) + \sin\delta_S\cos\phi_s\sin(\Delta m_s t))\right]$	$\frac{4}{3}\sqrt{3}\cos\psi_T\left(1-\sin^2\theta_T\cos^2\phi_T\right)$

Eur. Phys. J. C 81 (2021) 342

Lancaster University

CPV in $B^0_s \to J/\psi\phi$: OS Tagging

- Knowledge of the initial flavour can improve the precision of the CP-violation measurement.
- **Muon/electron tagging**: semi-leptonic decay of B (b→μ/e transition); momentum weighed charge of lepton and tracks in the cone ΔR < 0.5 around the leading lepton, (constant κ = 1.1).

$$Q_\ell = \frac{\sum_i^{N_{\text{tracks}}} q_i \, p_{\text{T}i}^{\kappa}}{\sum_i^{N_{\text{tracks}}} p_{\text{T}i}^{\kappa}}$$

- **b-jet-charge tagging**: used if the additional muon/electron is absent; momentum-weighted track-charge in jet.
- Self-tagging B→ J/ψ K± channel used for calibration and performance estimation.

Tag method	Efficiency [%]	Effective Dilution [%]	Tagging Power [%]
Tight muon	4.50 ± 0.01	43.8 ± 0.2	0.862 ± 0.009
Electron	1.57 ± 0.01	41.8 ± 0.2	0.274 ± 0.004
Low-p_T muon	3.12 ± 0.01	29.9 ± 0.2	0.278 ± 0.006
Jet	12.04 ± 0.02	16.6 ± 0.1	0.334 ± 0.006
Total	21.23 ± 0.03	28.7 ± 0.1	1.75 ± 0.01

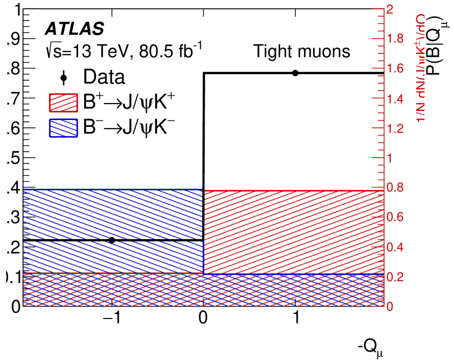

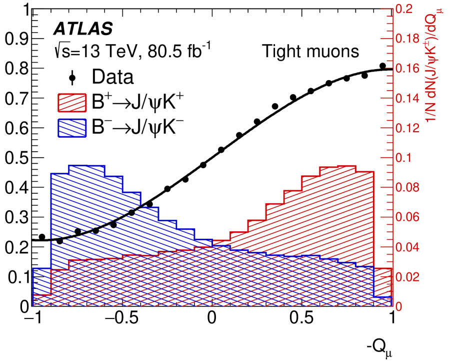

Eur. Phys. J. C 81 (2021) 342

Lancaster University

CPV in $B^0_s \rightarrow J/\psi\phi$: Fit

- Unbinned maximum likelihood (UML) fit performed to extract parameters of interest.
- Decay observables: mass, time, angles, per-candidate tagging and mass/time resolutions (pT(B) dependent).

$$\ln \mathcal{L} = \sum_{i=1}^{N} \left\{ w_i \cdot \ln \left(f_{\text{sig}} \cdot \mathcal{F}_{\text{sig}} + f_{\text{sig}} \cdot f_{B_d^0} \cdot \mathcal{F}_{B_d^0} + f_{\text{sig}} \cdot f_{\Lambda_b} \cdot \mathcal{F}_{\Lambda_b} + (1 - f_{\text{sig}}(1 + f_{B_d^0} + f_{\Lambda_b})) \cdot \mathcal{F}_{\text{bck}} \right) \right\}.$$

- Fixed parameters: Δm_s = PDG, no direct CP-violation assumed.
- Time inefficiency, modelled in MC: Trigger and reco effects.

Eur. Phys. J. C 81 (2021) 342

CPV in $B^0_s \rightarrow J/\psi\phi$: Fit

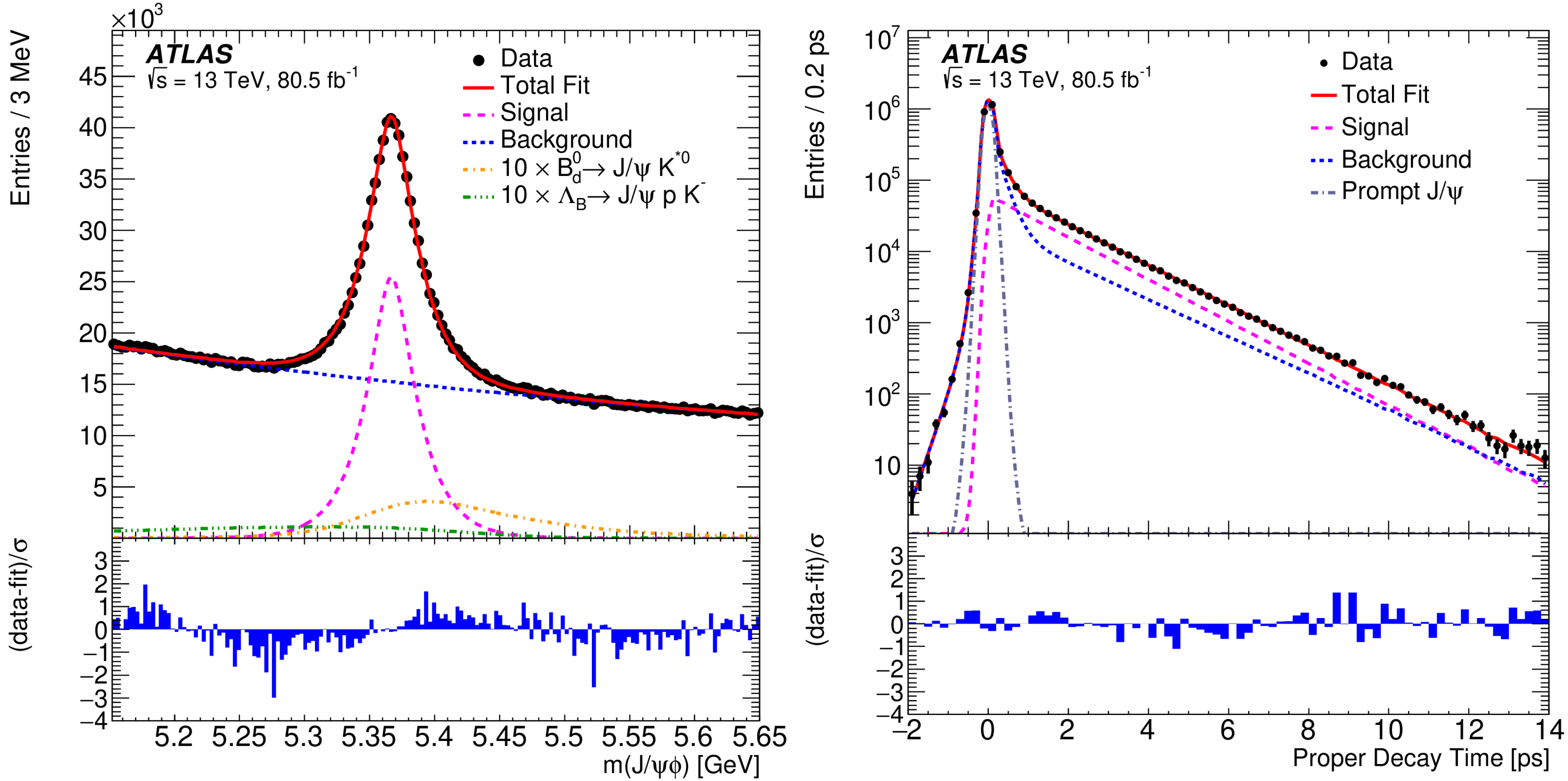

Ratio plots include both stat. and syst. uncertainties

CPV in $B^0_s \rightarrow J/\psi\phi$: Fit

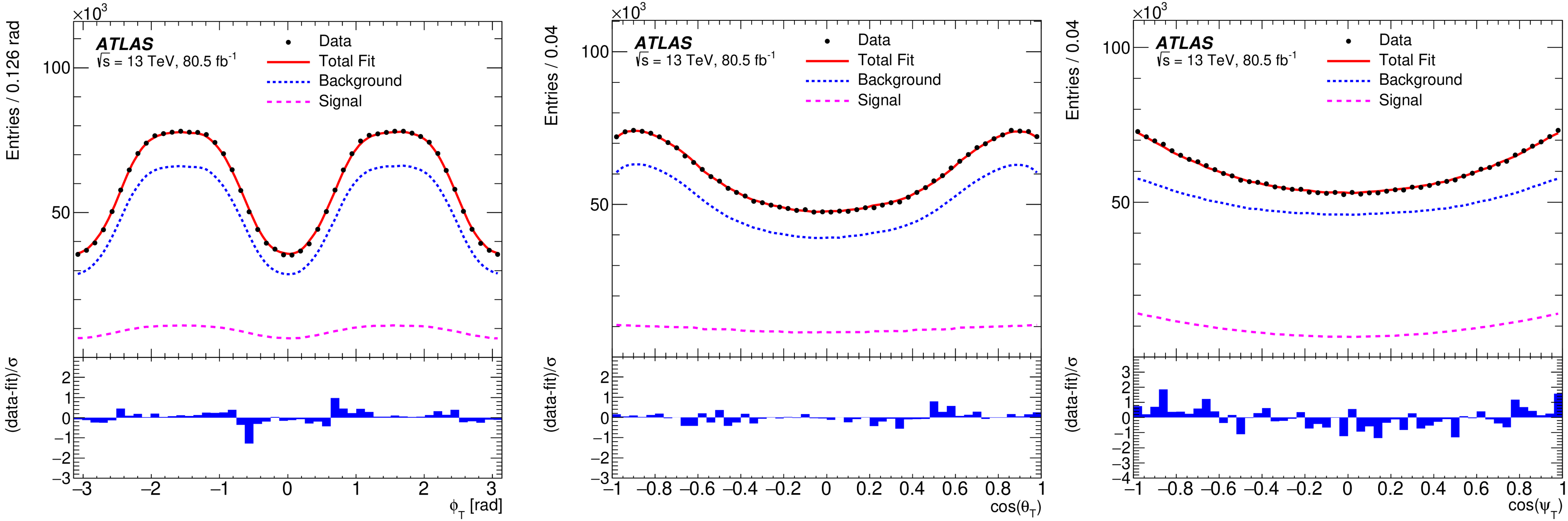

Ratio plots include both stat. and syst. uncertainties

Eur. Phys. J. C 81 (2021) 342

CPV in $B^0_s \rightarrow J/\psi\varphi$: Result

- Likelihood fit determined two solutions for the strong phases, but no effect on the result.

Parameter	Value	Statistical uncertainty	Systematic uncertainty
ϕ_s [rad]	−0.081	0.041	0.022
$\Delta\Gamma_s$ [ps^{-1}]	0.0607	0.0047	0.0043
Γ_s [ps^{-1}]	0.6687	0.0015	0.0022
$\|A_\parallel(0)\|^2$	0.2213	0.0019	0.0023
$\|A_0(0)\|^2$	0.5131	0.0013	0.0038
$\|A_S(0)\|^2$	0.0321	0.0033	0.0046
$\delta_\perp - \delta_S$ [rad]	−0.25	0.05	0.04
Solution (a)			
$\delta_\perp$ [rad]	3.12	0.11	0.06
$\delta_\parallel$ [rad]	3.35	0.05	0.09
Solution (b)			
$\delta_\perp$ [rad]	2.91	0.11	0.06
$\delta_\parallel$ [rad]	2.94	0.05	0.09

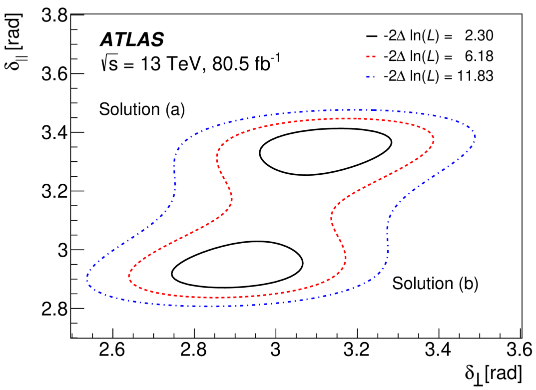

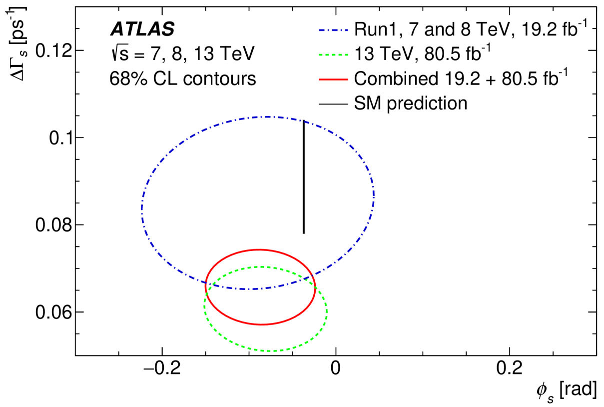

- Weak phase φ_s as well as decay width difference $\Delta\Gamma_s$ compatible with SM.
- Dominant systematics on φ_s measurement from tagging.
- Statistical (BLUE) combination with Run 1 result.

$$\{\delta_\parallel,\ \delta_\perp,\ \delta_S\} \rightarrow \{2(\pi - \delta_\parallel),\ \delta_\perp + (\pi - \delta_\parallel),\ \delta_\perp - \delta_S + (\pi - \delta_\parallel)\}.$$

CPV in $B^0_s \to J/\psi\phi$: Comparison

- ATLAS: Still 60 fb^{-1} of 2018 data to be added.
- HFLAV average for PDG 2021: $\varphi_s = -0.050 \pm 0.019$ rad.

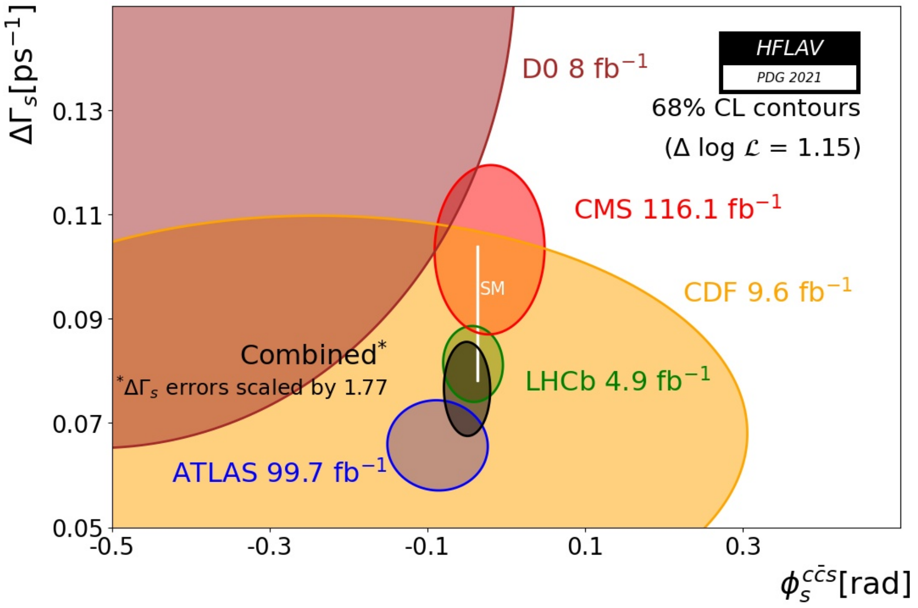

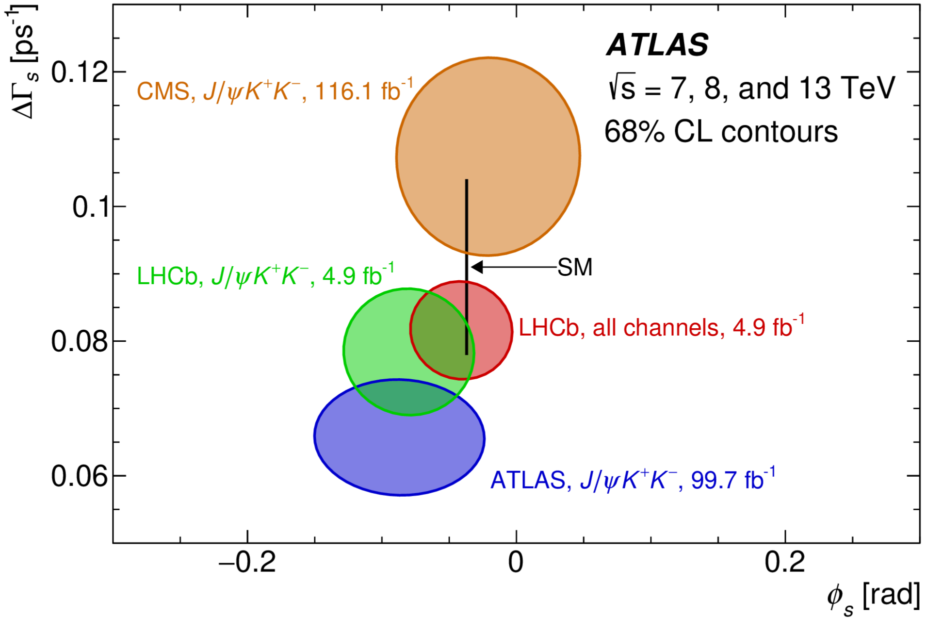

Lancaster University

Study of the rare decays of B_s^0 and B^0 mesons into muon pairs using data collected during 2015 and 2016 with the ATLAS detector

JHEP 04 (2019) 098

$B^0_s \to \mu\mu$: Introduction

- Flavour-changing neutral-current processes highly suppressed in the SM.
- NP can significantly contribute, modifying the branching ratio.
- 36.2 fb^{-1} dataset of 2015-2016 data taking, but effectively 26.3 fb^{-1} for $B^0_s \to \mu\mu$ (due to prescale).
- Lxy > 0 and m ϵ (4.0, 8.5) GeV requested at HLT.
- $\mathcal{B}(B^0_s \to \mu^+\mu^-)$ measurement relative to $B(B^\pm \to J/\psi K^\pm)$; $f_{u,d,s}$ are hadronisation probabilities of a b-quark:
- $B^0_s \to J/\psi\varphi$ is used as a control channel.
- Blinded signal di-muon invariant mass region (5166, 5526) MeV.
- BDT based background suppression, trained on sidebands data.
- Yields obtained from fit to mass spectra.
- Relative reconstruction efficiencies estimated from corrected MC.

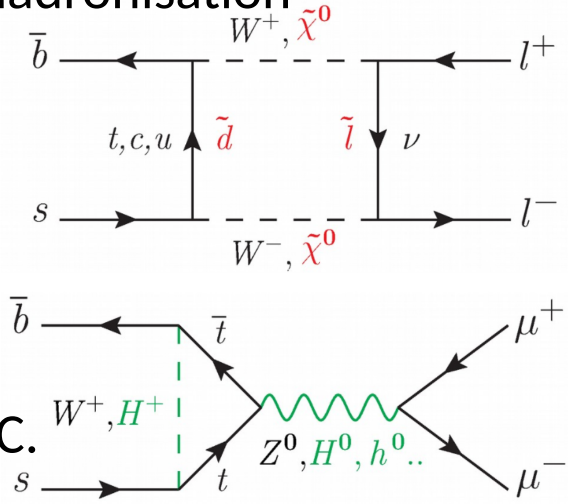

JHEP 04 (2019) 098

$B^0_s \rightarrow \mu\mu$: Background

- Partially reconstructed b-hadron decays:
  - Same Vertex: $B^0 \rightarrow \mu\mu X$ decays.
  - Same Side: $b \rightarrow c\mu X \rightarrow s(d)\mu X'$.
  - Semileptonic decay with misidentied hadron.
- Peaking backgrounds:
  - $B^0 \rightarrow h^+h^-$, both hadrons misidentied as muons.
  - Used tight muon criteria. Only 2.7 ± 1.3 events!
  - Simulated and fixed in the mass fit.
- Continuum background:
  - Combinatorics of muon and uncorrelated hadron decays.
  - Reduced by Boosted Decision Tree (BDT) classifier. Linear shape constrained in the mass fit across BDT bins.

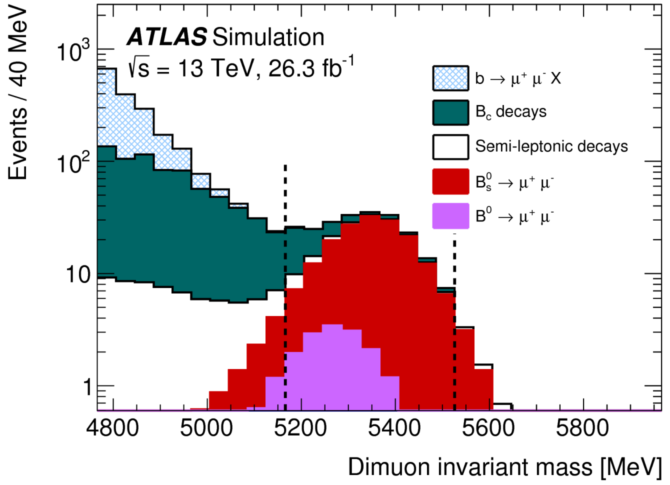

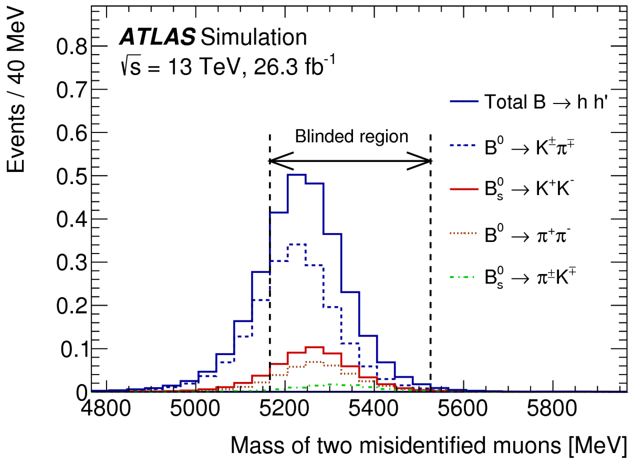

JHEP 04 (2019) 098

$B^0_s \to \mu\mu$: BDT and signal extraction

- Signal region divided into four Boosted Decision Tree bins with constant signal efficiency.
- 15 BDT variables (kinematics, isolation, B-vertex separation from PV).
- Validated on $B^\pm \to J/\psi\, K^\pm$ and $B_s^0 \to J/\psi\, \varphi$ channels.
- Simultaneous UML fit to di-muon mass distributions in the four BDT bins to extract yield.
- Signal model from MC, two double Gaussians, centred on $B^0{}_s$ masses.
- Unconstrained yields: $N_s = 80 \pm 22$ and $N_d = -12 \pm 20$. (Expected N_s=90, N_d=10).
- Contour obtained using Neyman construction.
- Run 1 + 2015 + 2016 combined within 2.4 σ of SM. Stat limited.

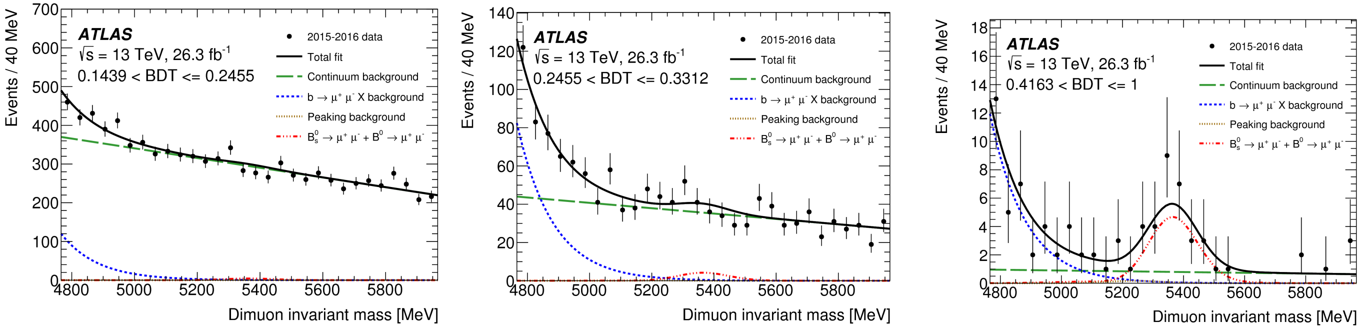

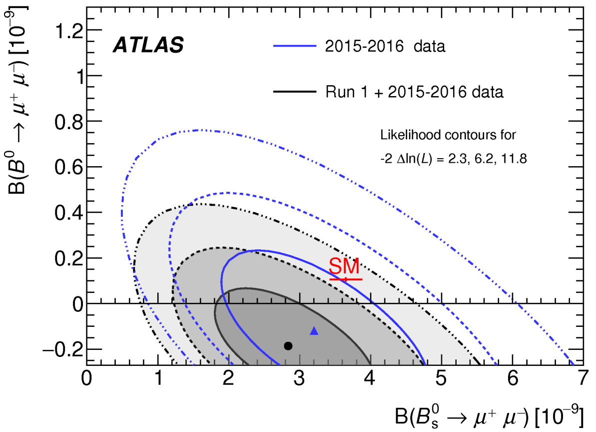

ATLAS-CONF-2020-049

$B^0_s \rightarrow \mu\mu$: LHC Combination

- ATLAS, CMS and LHCb results.
- Combination from binned 2D profile likelihood.
- Independent systematics, except for the ratio of fragmentation fractions $\frac{f_d}{f_s}$

	LHC	SM
$\mathcal{B}(B^0_s \rightarrow \mu\mu)\ [10^{-9}]$	$2.69^{+0.37}_{-0.35}$	3.66 ± 0.14
$\mathcal{B}(B^0 \rightarrow \mu\mu)\ [10^{-10}]$	< 1.9 at 95% CL	1.03 ± 0.05

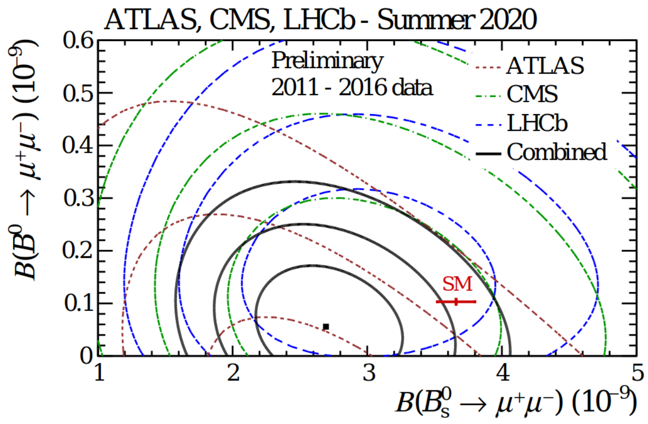

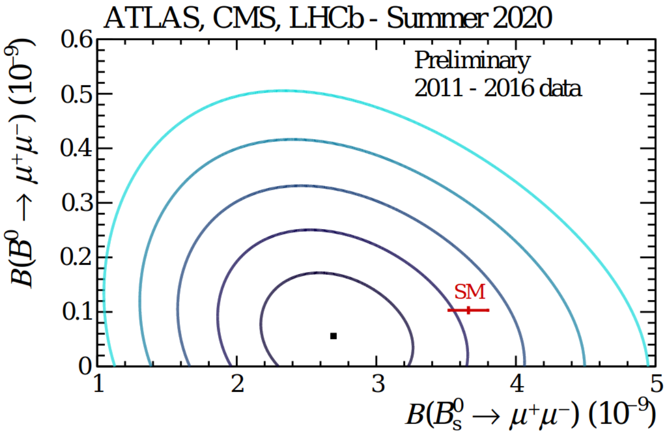

Prospects of CPV Measurements

Lancaster University

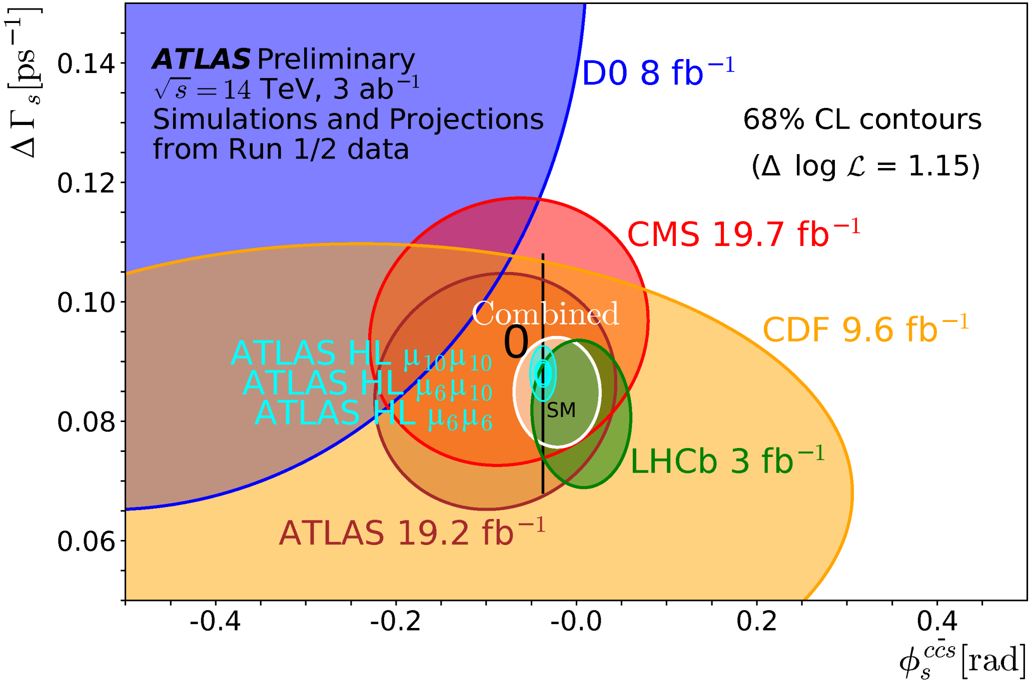

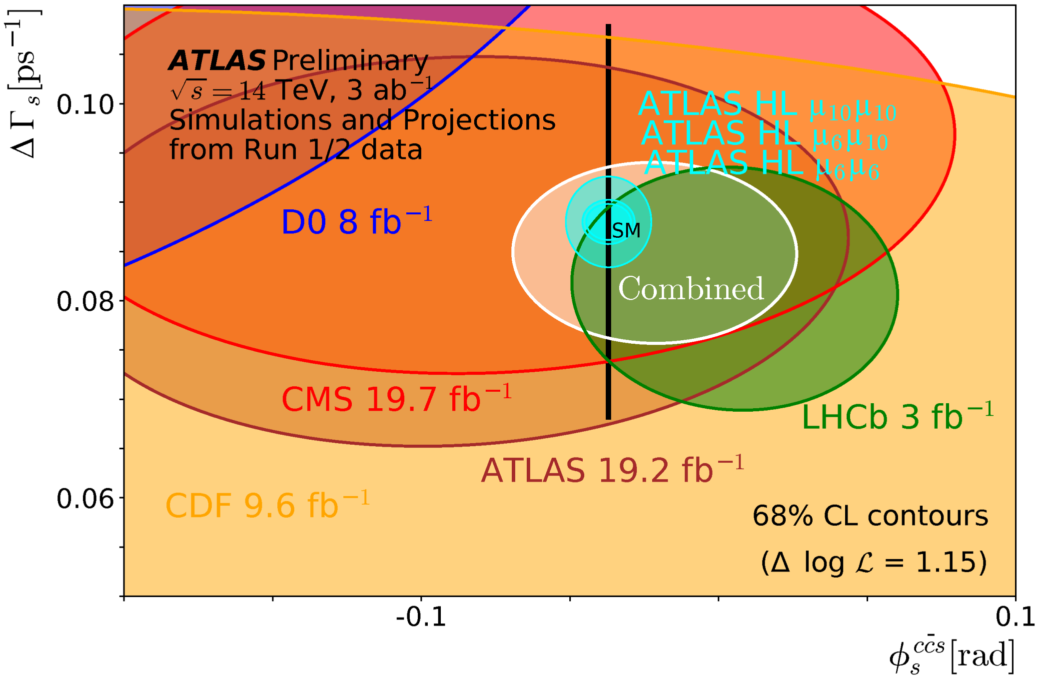

ATLAS and CMS Collaborations, Report on the Physics at the HL-LHC and Perspectives for the HE-LHC, arXiv:1902.10229

Lancaster University

ATLAS HL-LHC prospects for semi-rare decay $B \to \mu^+\mu^- K^*$

ATLAS HL-LHC measurement precision in the P4 and P5 parameters is estimated using Toy-MC simulations and consequent fit to the decay angular distributions.

3 trigger scenarios for thresholds: muon p_T

Scenarios modelled: Conservative (10-10) GeV (x5 Run1); Intermediate (6-10) GeV (x8 Run1); High-yield (6-6) GeV (x9 Run1).

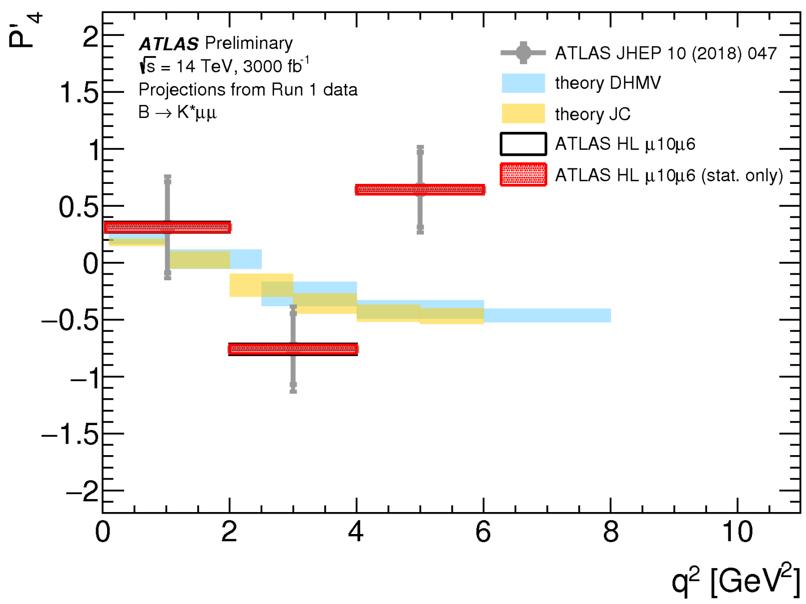

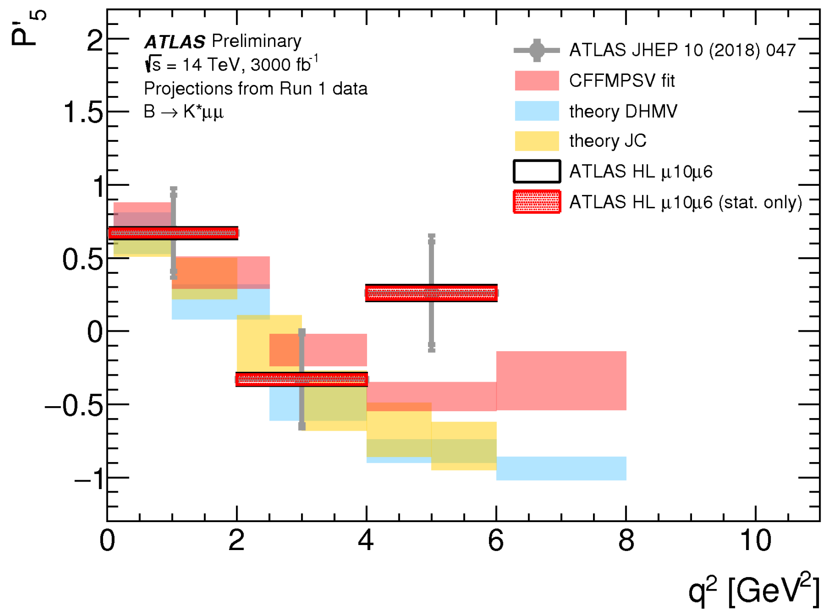

Summary

- ATLAS has competitive results in B-physics.
- Working on the updates to the mentioned analysis to full Run-2 statistics.
- BLS group is well prepared for run 3 data.
- More public results on ATLAS B-physics TWiki page:

  https://twiki.cern.ch/twiki/bin/view/AtlasPublic/BPhysPublicResults

Backup

k	$\mathcal{O}^{(k)}(t)$	$g^{(k)}(\theta_T, \psi_T, \phi_T)$
1	$\frac{1}{2}\|A_0(0)\|^2\left[(1+\cos\phi_s)\,e^{-\Gamma_L^{(s)}t}+(1-\cos\phi_s)\,e^{-\Gamma_H^{(s)}t}\pm 2e^{-\Gamma_s t}\sin(\Delta m_s t)\sin\phi_s\right]$	$2\cos^2\psi_T(1-\sin^2\theta_T\cos^2\phi_T)$
2	$\frac{1}{2}\|A_\parallel(0)\|^2\left[(1+\cos\phi_s)\,e^{-\Gamma_L^{(s)}t}+(1-\cos\phi_s)\,e^{-\Gamma_H^{(s)}t}\pm 2e^{-\Gamma_s t}\sin(\Delta m_s t)\sin\phi_s\right]$	$\sin^2\psi_T(1-\sin^2\theta_T\sin^2\phi_T)$
3	$\frac{1}{2}\|A_\perp(0)\|^2\left[(1-\cos\phi_s)\,e^{-\Gamma_L^{(s)}t}+(1+\cos\phi_s)\,e^{-\Gamma_H^{(s)}t}\mp 2e^{-\Gamma_s t}\sin(\Delta m_s t)\sin\phi_s\right]$	$\sin^2\psi_T\sin^2\theta_T$
4	$\frac{1}{2}\|A_0(0)\|\|A_\parallel(0)\|\cos\delta_\parallel\left[(1+\cos\phi_s)\,e^{-\Gamma_L^{(s)}t}+(1-\cos\phi_s)\,e^{-\Gamma_H^{(s)}t}\pm 2e^{-\Gamma_s t}\sin(\Delta m_s t)\sin\phi_s\right]$	$\frac{1}{\sqrt{2}}\sin 2\psi_T\sin^2\theta_T\sin 2\phi_T$
5	$\|A_\parallel(0)\|\|A_\perp(0)\|\left[\frac{1}{2}(e^{-\Gamma_L^{(s)}t}-e^{-\Gamma_H^{(s)}t})\cos(\delta_\perp-\delta_\parallel)\sin\phi_s\pm e^{-\Gamma_s t}(\sin(\delta_\perp-\delta_\parallel)\cos(\Delta m_s t)-\cos(\delta_\perp-\delta_\parallel)\cos\phi_s\sin(\Delta m_s t))\right]$	$-\sin^2\psi_T\sin 2\theta_T\sin\phi_T$
6	$\|A_0(0)\|\|A_\perp(0)\|\left[\frac{1}{2}(e^{-\Gamma_L^{(s)}t}-e^{-\Gamma_H^{(s)}t})\cos\delta_\perp\sin\phi_s\pm e^{-\Gamma_s t}(\sin\delta_\perp\cos(\Delta m_s t)-\cos\delta_\perp\cos\phi_s\sin(\Delta m_s t))\right]$	$\frac{1}{\sqrt{2}}\sin 2\psi_T\sin 2\theta_T\cos\phi_T$
7	$\frac{1}{2}\|A_S(0)\|^2\left[(1-\cos\phi_s)\,e^{-\Gamma_L^{(s)}t}+(1+\cos\phi_s)\,e^{-\Gamma_H^{(s)}t}\mp 2e^{-\Gamma_s t}\sin(\Delta m_s t)\sin\phi_s\right]$	$\frac{2}{3}\left(1-\sin^2\theta_T\cos^2\phi_T\right)$
8	$\alpha\|A_S(0)\|\|A_\parallel(0)\|\left[\frac{1}{2}(e^{-\Gamma_L^{(s)}t}-e^{-\Gamma_H^{(s)}t})\sin(\delta_\parallel-\delta_S)\sin\phi_s\pm e^{-\Gamma_s t}(\cos(\delta_\parallel-\delta_S)\cos(\Delta m_s t)-\sin(\delta_\parallel-\delta_S)\cos\phi_s\sin(\Delta m_s t))\right]$	$\frac{1}{3}\sqrt{6}\sin\psi_T\sin^2\theta_T\sin 2\phi_T$
9	$\frac{1}{2}\alpha\|A_S(0)\|\|A_\perp(0)\|\sin(\delta_\perp-\delta_S)\left[(1-\cos\phi_s)\,e^{-\Gamma_L^{(s)}t}+(1+\cos\phi_s)\,e^{-\Gamma_H^{(s)}t}\mp 2e^{-\Gamma_s t}\sin(\Delta m_s t)\sin\phi_s\right]$	$\frac{1}{3}\sqrt{6}\sin\psi_T\sin 2\theta_T\cos\phi_T$
10	$\alpha\|A_0(0)\|\|A_S(0)\|\left[\frac{1}{2}(e^{-\Gamma_H^{(s)}t}-e^{-\Gamma_L^{(s)}t})\sin\delta_S\sin\phi_s\pm e^{-\Gamma_s t}(\cos\delta_S\cos(\Delta m_s t)+\sin\delta_S\cos\phi_s\sin(\Delta m_s t))\right]$	$\frac{4}{3}\sqrt{3}\cos\psi_T\left(1-\sin^2\theta_T\cos^2\phi_T\right)$